# Accelerated fat cell aging links oxidative stress and insulin resistance in adipocytes

Finny Monickaraj, Sankaramoorthy Aravind, Pichamoorthy Nandhini, Paramasivam Prabu, Chandrakumar Sathishkumar, Viswanathan Mohan and Muthuswamy Balasubramanyam*

*Madras Diabetes Research Foundation and Dr. Mohan's Diabetes Specialities Centre, WHO Collaborating Centre for Non-Communicable Diseases Prevention and Control, IDF Centre of Education, Gopalapuram, Chennai 600 086, India*

**Corresponding author (Fax, 9144-2835-0935; Email, balusignal@gmail.com; drbalu@mdrf.in)*

Telomere shortening is emerging as a biological indicator of accelerated aging and aging-related diseases including type 2 diabetes. While telomere length measurements were largely done in white blood cells, there is lack of studies on telomere length in relation to oxidative stress in target tissues affected in diabetes. Therefore, the aim of this study is to induct oxidative stress in adipocytes and to test whether these adipocytes exhibit shortened telomeres, senescence and functional impairment. 3T3-L1 adipocytes were subjected to oxidative stress and senescence induction by a variety of means for 2 weeks (exogenous application of $H_2O_2$, glucose oxidase, asymmetric dimethylarginine (ADMA) and glucose oscillations). Cells were probed for reactive oxygen species generation (ROS), DNA damage, mRNA and protein expression of senescent and pro-inflammatory markers, telomere length and glucose uptake. Compared to untreated cells, both ROS generation and DNA damage were significantly higher in cells subjected to oxidative stress and senescence. Adipocytes subjected to oxidative stress also showed shortened telomeres and increased mRNA and protein expression of p53, p21, TNFα and IL-6. Senescent cells were also characterized by decreased levels of adiponectin and impaired glucose uptake. Briefly, adipocytes under oxidative stress exhibited increased ROS generation, DNA damage, shortened telomeres and switched to senescent/pro-inflammatory phenotype with impaired glucose uptake.

[Monickaraj F, Aravind S, Nandhini P, Prabu P, Sathishkumar C, Mohan V and Balasubramanyam M 2013 Accelerated fat cell aging links oxidative stress and insulin resistance in adipocytes. *J. Biosci.* **38** 113–122] **DOI** 10.1007/s12038-012-9289-0

## 1. Introduction

Adipose tissue is no longer considered only an energy storage organ. Recent studies imply that fat tissue is at the nexus of mechanisms and pathways involved in longevity, genesis of age-related diseases, inflammation and metabolic dysfunction (Tchkonia *et al.* 2010). Excess or dysfunctional fat tissue appears to accelerate onset of multiple age-related diseases, while interventions that delay or limit fat tissue turnover, redistribution or dysfunction in experimental animals are associated with enhanced health span and maximum lifespan. Metabolic disorders like obesity, type 2 diabetes and cardiovascular disorders synchronize with aging process in their onset and progression. Hence, aging has been considered as one of the factors contributing in accelerating the development and progression of metabolic syndrome in individuals with the risk (Arai *et al.* 2011; Guarner-Lans *et al.* 2011). In obese condition, which is also a state of fat tissue aging, adipose tissue secretes high levels of pro-inflammatory cytokines, which alter the normal metabolic process, leading to inflammation and insulin resistance (Hotamisligil *et al.* 1993; Weisberg *et al.* 2003; Kamei *et al.* 2006). It is also known that adipose tissue of obese undergo accelerated senescence leading to further secretion

**Keywords.** Adipocytes; insulin resistance; oxidative stress; p53; senescence

Abbreviations used: ADMA, asymmetric; $N^G$, $N^G$-dimethylarginine; FBS, fetal bovine serum; GO, glucose oxidase; $H_2O_2$, hydrogen peroxide; IBMX, iso-butyl methyl xanthine; ROS, reactive oxygen species; SA-β-gal, senescence-associated β-galactosidase



Published online: 8 January 2013

of inflammatory cytokines (Campisi 2005; Minamino and Komuro 2007). Since cellular senescence leads to a senescent secretory phenotype with increased inflammatory cytokines and detrimental microenvironment, it is important to study the cellular and molecular mechanisms of accelerated senescence in the context of increasing epidemic of metabolic diseases.

Biologically accelerated aging occurs due to cellular senescence as a result of metabolically induced abnormalities like reactive oxygen species (ROS) generation, DNA damage and telomere shortening (Lu and Finkel 2008). ROS generation as a result of oxidative stress has been implicated in the development of insulin resistance and type 2 diabetes (Mehta *et al.* 2006). Biomarkers of oxidative stress and shortened telomeres were shown associated with age-related diseases including type 2 diabetes (Adaikalakoteswari *et al.* 2005; Sampson *et al.* 2006; Balasubramanyam *et al.* 2007; Salpea *et al.* 2010; Monickaraj *et al.* 2012). While an association of oxidative stress and telomere shortening was studied largely in white blood cells, there is hardly any data that reveals whether this phenomenon reflects in target tissues affected in diabetes. There is an imperative need to study the cell biological and molecular mechanisms that determine how oxidative stress and accelerated senescence impacts fat tissue function and how this, in turn, leads to age-related disease. With this background, the present study is attempted to impose oxidative stress (by a variety of cell stressors) in adipocytes and to investigate the alterations in senescence markers with special reference to telomere shortening, p53 up-regulation, pro-inflammation and insulin-stimulated glucose uptake.

## 2. Materials and methods

### 2.1 *Cell culture*

3T3-L1 preadipocytes were cultured in Dulbecco's Modified Eagle's Medium (DMEM) under standard tissue culture conditions. 3T3-L1 cells were differentiated by using a mixture of IBMX, insulin and dexamethasone with 10% FBS for first 3 days and subsequently with 10 nM insulin and 10% FBS by replenishing the medium every 2 days for 10–14 days.

### 2.2 *Treatment of cells and induction of oxidative stress*

Four different experimental maneuvers have been adopted to induct oxidative stress in adipocytes: (i) Cells were treated with 100 μM $H_2O_2$ for 2 h in serum-free medium, passaged and allowed to grow till confluent. Cells were again pulsed with 100 μM $H_2O_2$ for 2 h at each passage and this treatment was continued for 14 days. (ii) $H_2O_2$ was generated intracellularly by incubating the cells with 10 mU/ml of glucose oxidase (type 2 from *Aspergillus niger*; Sigma) in the presence of 25 mM glucose for 2 h in serum-free medium but with 0.5% of bovine serum albumin (BSA). Glucose oxidase treatment was done at each passage similar to $H_2O_2$ application regimen. (iii) Cells were treated with 100 μM ADMA (asymmetric $N^G$, $N^G$-dimethylarginine) for 14 days by replacing the media after every 48 h. (iv) To mimic and simulate the glucose excursions seen in diabetic patients, cells were imposed to high glucose/low glucose (HG-LG) switch where cells were exposed to high glucose (30 mM) and low glucose (5 mM) on every alternate passage till 14 days.

### 2.3 *Senescence-associated β-galactosidase staining*

Briefly, cells were cultured in six-well plate and after the end of the specific treatment period, cells were washed once with 2 mL of 1× PBS and fixed with 1 mL fixative solution for 10–15 min at room temperature. Cells were washed twice with 2 mL of 1× PBS and 1 ml of β-Galactosidase Staining Solution was added to the plate and incubated overnight at 37°C. Cells were observed under microscope (40× magnification) in 4 different fields. SA-β-gal-positive cells were quantified by counting stained and unstained cells and expressed as the percent of SA-β-gal-positive cells over the total counted.

### 2.4 *ROS measurement*

Intracellular ROS generation was measured using DCF-DA dye method. Once the cells were treated according to the experimental conditions, cells were incubated with 15 μM DCF-DA for 45 min, briefly centrifuged down to remove the dye and resuspended in HEPES buffer. The change in fluorescence was measured in a spectrofluorimeter set at 485 nm excitation and 530 nm emission. Cells were challenged with PMA to induct ROS generation. Change in fluorescence intensity was represented in arbitrary units.

### 2.5 *Comet assay or single cell gel electrophoresis (DNA damage assessment)*

DNA damage was assessed by comet assay (Singh *et al.* 1988; Adaikalakoteswari *et al.* 2007). Briefly, $10^4$ cells were washed briefly with cold PBS and scraped and suspended in 200 μL of 0.5% low-melting agarose, after which cells were layered over microscopic slide precoated with 1% agarose. The slides were then immersed and incubated in Lysis buffer (2.5 M NaCl, 100 mM EDTA, 10 mM Tris pH 10, 10% DMSO and 1% Trion X-100) for 1 h at 4°C. Slides were transferred into DNA electrophoresis tank containing

electrophoresis buffer (1 mM EDTA, 300 mM NaOH, pH 13) and incubated for 20 min, after which electrophoresis was carried out for 20 min at 200 mV. At the end of the electrophoresis run, slides were soaked in neutralizing buffer (400 mM Tris, pH 7.5) for 15 min and stained with ethidium bromide (20 μg/mL) and analysed under fluorescent microscope. The amount of DNA damage was calculated using Comet Imager 2.1. The data were represented as % DNA damage.

### 2.6 *Telomere length measurement by real-time PCR*

Relative telomere length was determined by real-time PCR as previously described (Cawthon 2002). Relative telomere length was measured by real-time PCR using genomic DNA obtained from cells under different treatment conditions. This method measures the factor by which the ratio of telomere repeat copy number to single-gene copy number differs between a sample and that of a reference DNA sample. PCR amplification was achieved using telomere (T) and single copy gene, 36B4 (encodes acidic ribosomal phosphoprotein) primers (S) which serves as a quantitative control. The mean telomere repeat gene sequence (T) to a reference single copy gene (S) is represented as T/S ratio, which was calculated to determine the relative telomere length. Briefly, PCR reactions were performed in triplicate in 20 μL reaction volumes (using 25 ng DNA sample per reaction) for all the samples studied. The PCR mixture contained 10 pmol of each of the primers, 100 μM of each dNTPs and 0.3× SYBR green dye and 0.5 Units of fast Taq DNA polymerase (Fermentas, USA). The PCR thermal conditions for relative telomere length assay using telomeric primers (T) and single copy gene primers (S) consisted of a initial denaturation of 5 min at 95°C, followed by a total of 40 cycles at 95°C for 5 s, 56°C for 30 s, and 72°C for 30 s and fluorescence acquisition. Crossing points (Cp) were determined using the ABI 7000. A standard curve derived from serially diluted reference DNA was generated in order to check PCR efficiency between the plates. The average of telomere versus single copy gene (T/S) ratio was calculated, which is proportional to telomere length of each individual. For quality control purposes, we repeated many samples that were separately PCR amplified.

### 2.7 *mRNA quantification by real-time PCR*

Total RNA from cells was isolated and converted to cDNA as described previously (Balasubramanyam *et al.* 2011). Quantitative real-time PCR was performed for specific genes using SYBR green master mix (Finnzymes). PCR amplification was carried out using ABI-7000 (Applied Biosystems) with appropriate cycle conditions. The expression level of RNA was determined using $2^{-DDCt}$ and normalized using β-actin. The primer sequences of specific genes are listed in table 1.

### 2.8 *Protein extraction and Western blot*

Cells were washed with cold PBS thrice and scraped into 100 μL RIPA buffer (25 mM Tris HCl pH 7.6, 150 mM NaCl, 1 mM EGTA, 1% triton-X 100, 1% sodium deoxy cholate, 1% SDS and 1 μg/mL leupeptin), sonicated and centrifuged at 12,000*g* for 15 min. Then, the supernatant was collected and the protein was quantified using Nano drop. Aliquots of 50 μg protein were added to gel loading buffer (5×), proteins were separated in 10% SDS-PAGE run and then Western blot was performed. Blots were then probed with specific antibodies of the protein of interest (such as p53, p21, IL-6, TNFα and adiponectin) followed by appropriate secondary antibody tagged with alkaline phosphatase and the blots were developed by NBT/BCIP

**Table 1.** Gene-specific primers

| Gene name | Primer Sequence |
|---|---|
| Telomere | Forward: CGG TTT GTT TGG GTT TGG GTT TGG GTT TGG GTT TGG GTT |
| | Reverse: GGC TTG CCT TAC CCT TAC CCT TAC CCT TAC CCT TAC CCT |
| Adiponectin | Forward: CTC CTC ATT TCT GTC TGT ACG |
| | Reverse: AGC TCT TCA GTT GTA GTA ACG |
| TNFα | Forward: TAC TTT GGA GTC ATT GCT CTG |
| | Reverse: CTA AGT TAG AAG GAT ACA GAC TGG |
| IL6 | Forward: TTC CAT CCA GTT GCC TTC TTG G |
| | Reverse: GTG GTA TAG ACA GGT CTG TTG GG |
| p53 | Forward: TTC TGT AGC TTC AGT TCA TTG G |
| | Reverse: ATG GCA GTC ATC CAG TCT TC |
| p21 | Forward: TGC ATC CGT TTC ACC CAA CC |
| | Reverse: CTC ATT TTT CCA AAG TGC TAT TCA GG |
| TERT | Forward: TTA GGT TCT TAC AAC AGA TCA AGA GC |
| | Reverse: GTA CTG GTG AGA CTC AGA TGC C |
| β-actin | Forward: ACC TTC TAC AAT GAG CTG CG |
| | Reverse: CTG GAT GGC TAC GTA CAT GG |
| 36B4 | Forward: TGA CAT CGT CTT TAA ACC CCG |
| | Reverse: TGT CTG CTC CCA CAA TGA AG |
| β-gal | Forward: TAT GAG CCA CAG CCC ACC AG |
| | Reverse: TGA ATG ACT TCT CGA AGA GCA AAA TAC |

method. β-actin was probed as internal control and used in ratio calculations.

### 2.9 *Determination of 2-deoxyglucose uptake*

After serum starvation, cells were washed thrice with Krebs-Ringer phosphate (KRH) buffer (10 mM phosphate buffer, pH 7.4, 136 mM NaCl, 4.7 mM KCl, 1.25 mM $MgSO_4$) and stimulated with 2 nM insulin for 15 min. Cells were again washed thrice with KRH buffer and incubated with 2-($^3$H)-deoxyglucose (0.1 mM, 0.5 μCi/mL) for 45 min. Once glucose uptake is facilitated, the cells were washed with cold PBS, treated with 0.1% SDS and kept for overnight incubation at room temperature. The cell-associated radioactivity was read using liquid scintillation counter. The data are represented as insulin-stimulated glucose uptake in percentage.

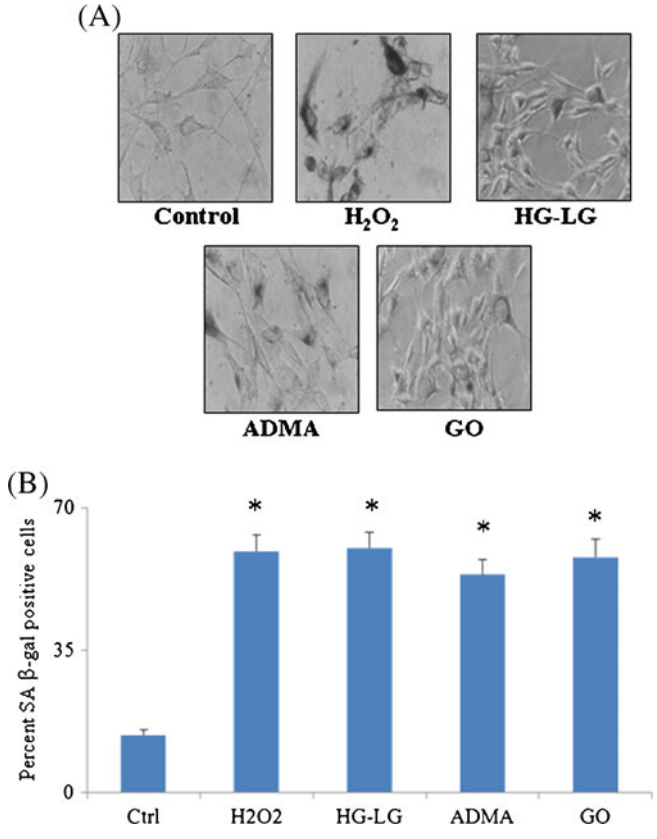


**Figure 1.** Induction of senescence as revealed by SA-β-gal staining from 3T3-L1 adipocytes under different experimental conditions. (**A**) Microscopic image of 3T3-L1-stained adipocytes in untreated cells and in cells treated with 100 μM hydrogen peroxide ($H_2O_2$) or high glucose and low glucose switch (HG-LG) or 100 μM asymmetric dimethylarginine (ADMA) or 10 mU/mL glucose oxidase (GO). Test conditions are the same in the subsequent figures. (**B**) Cumulative data on percent SA-β-gal positive cells. *$p<0.05$ compared to control.

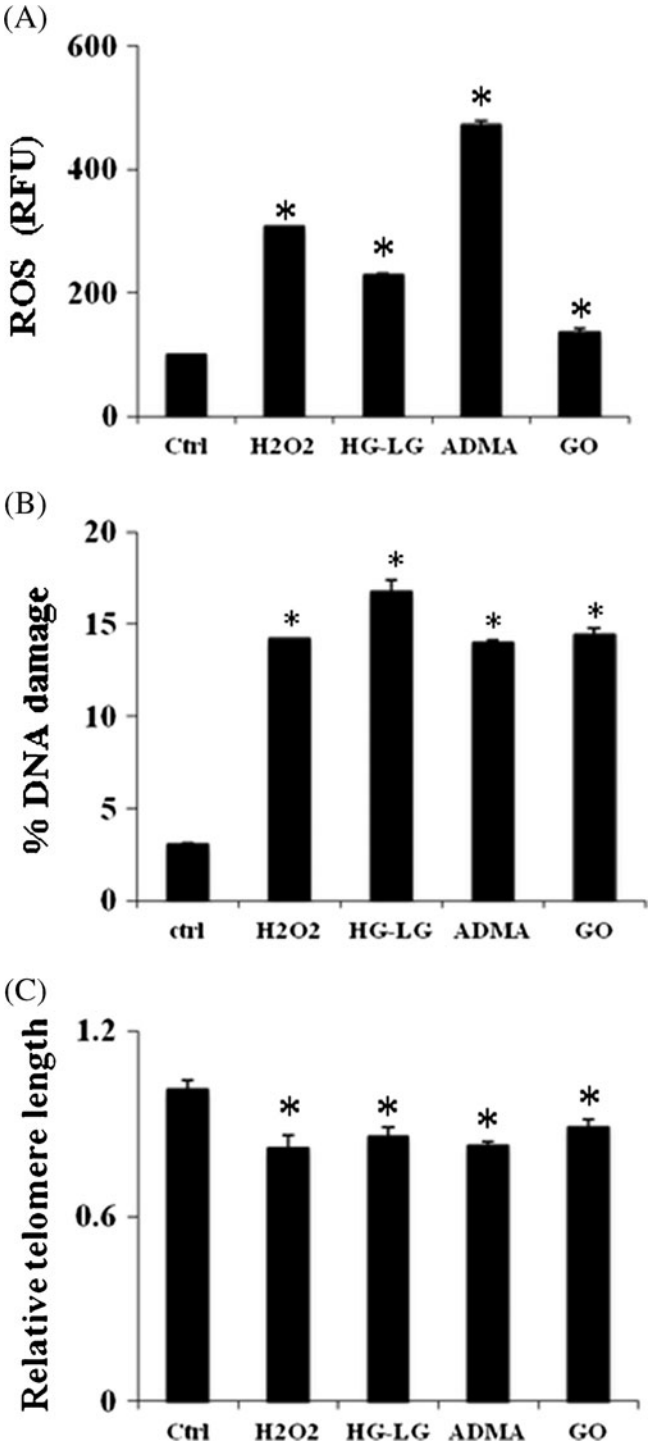


**Figure 2.** Cumulative data on ROS generation (relative fluorescence unit, RFU) (**A**), percentage DNA damage (**B**) and telomere length (**C**) measurements (mean±SE) in 3T3-L1 adipocytes under different experimental conditions (as mentioned in the legends to figure 1). *$p<0.05$ compared to control.

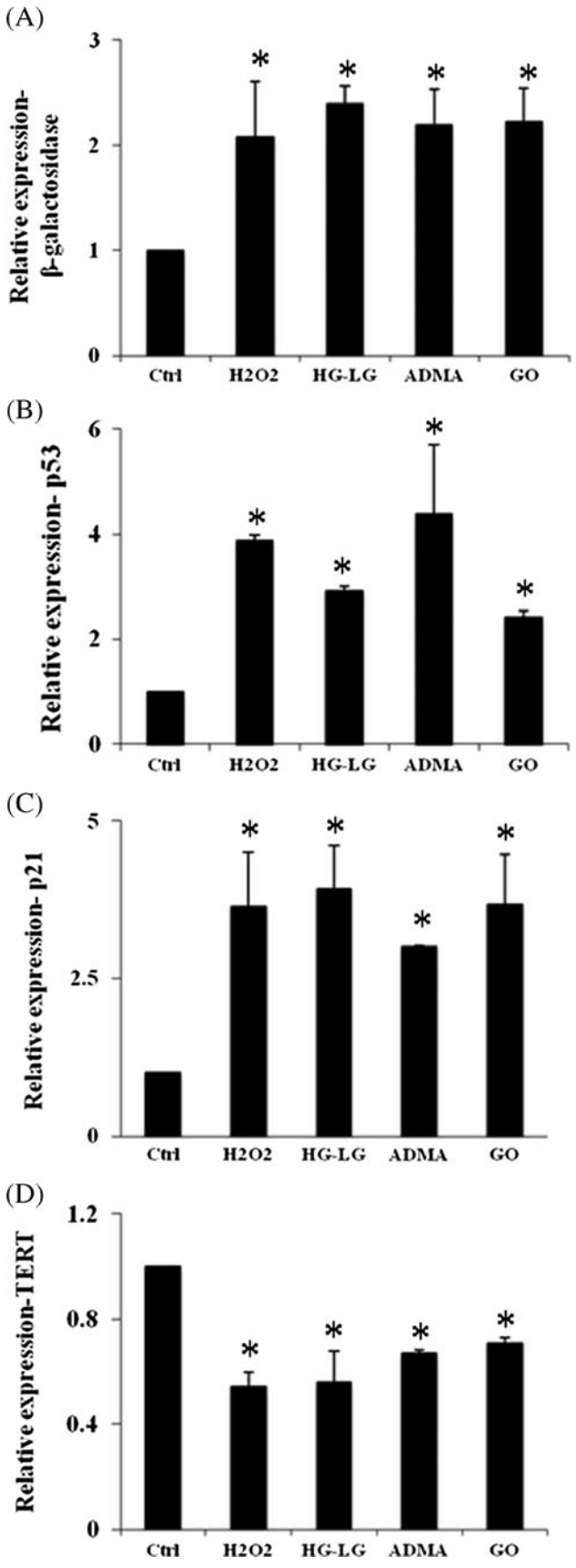


**Figure 3.** Real-time PCR gene expression patterns (mean±SE) of senescent markers, viz β-galactosidase (**A**), p53 (**B**), p21 (**C**) and gene expression levels of TERT (**D**) from 3T3-L1 adipocytes under different experimental conditions. *$p<0.01$ compared to control.

### 2.10 *Statistical analysis*

All measurements were performed under identical conditions for at least three times. All analysis was done using windows based SPSS statistical package (version 12.0, Chicago, IL). Data are subjected to ANOVA with $p<0.05$ as the criterion for significance.

## 3. Results

Compared to control cells, adipocytes treated with 100 μM $H_2O_2$ or high glucose/low glucose switch (5 mM – 30 mM – 5 mM) or 100 μM ADMA or 10 mU glucose oxidase in the presence of 25 mM glucose – all exhibited senescence as evidenced by increased SA-β-gal staining (figure 1A). The histogram in the figure 1B reveals the percent SA-β-gal-positive cells under treatment conditions.

Since four different experimental maneuvers were attempted to induct oxidative stress in adipocytes, first we tested whether these conditions resulted in increased generation of ROS. Figure 2A shows the extent of ROS generation under the study conditions. Compared to control cells, cells treated for oxidation and senescence exhibited significantly increased ($p<0.05$) generation of ROS. Since ROS could damage DNA, we next looked at the extent of DNA damage under various test conditions. In consonance with the increased generation of ROS, cells treated with various test agents also showed significantly ($p<0.05$) increased DNA damage (figure 2B). While ROS attack all biological molecules such as lipids, proteins and bulk of the chromosome, it was known that the telomeres with the TTAGGG repeats are more susceptible to ROS-induced damage. Therefore, we have measured telomere length in adipocytes subjected to different experimental maneuvers. Interestingly, those cells which were imposed to oxidative stress also exhibited significantly ($p<0.05$) shortened telomeres compared to control cells (figure 2C).

Because increased stress due to ROS can induce DNA damage and subsequent activation of senescent markers, we tested the mRNA and protein expression of several senescence signals (figures 3 and 4). Adipocytes exposed to oxidative stress showed increased mRNA expression of β-galactosidase (figure 3A), p53 (figure 3B) and p21 (figure 3C). Because TERT, the catalytic subunit of telomerase, is a negative regulator of DNA damage and stress responses, we then looked at the mRNA expression of TERT. Cells imposed to oxidative stress revealed decreased mRNA levels of TERT (figure 3D). Representative protein

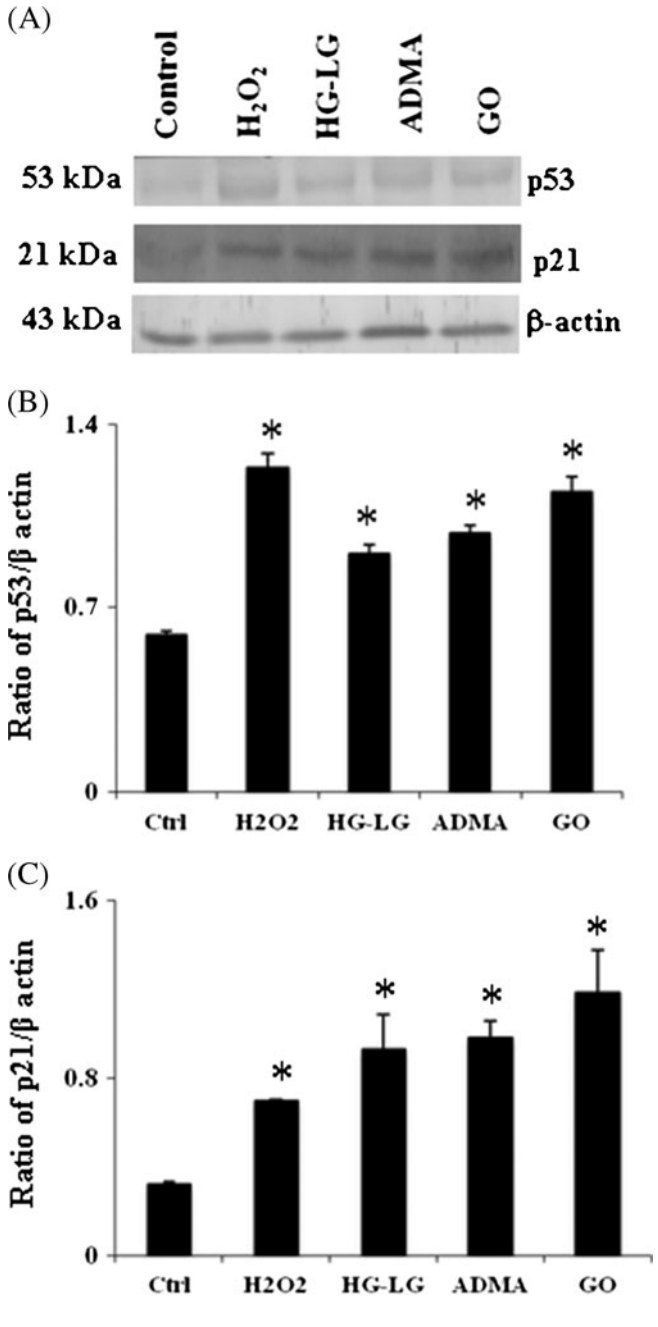


**Figure 4.** Protein expression patterns of senescent markers. (**A**) Representative protein expression blots of senescent markers along with β-actin. Cumulative protein expression data (mean±SE) of p53 (**B**) and p21 (**C**) signals from 3T3-L1 adipocytes under different experimental conditions. *$p<0.05$ compared to control.

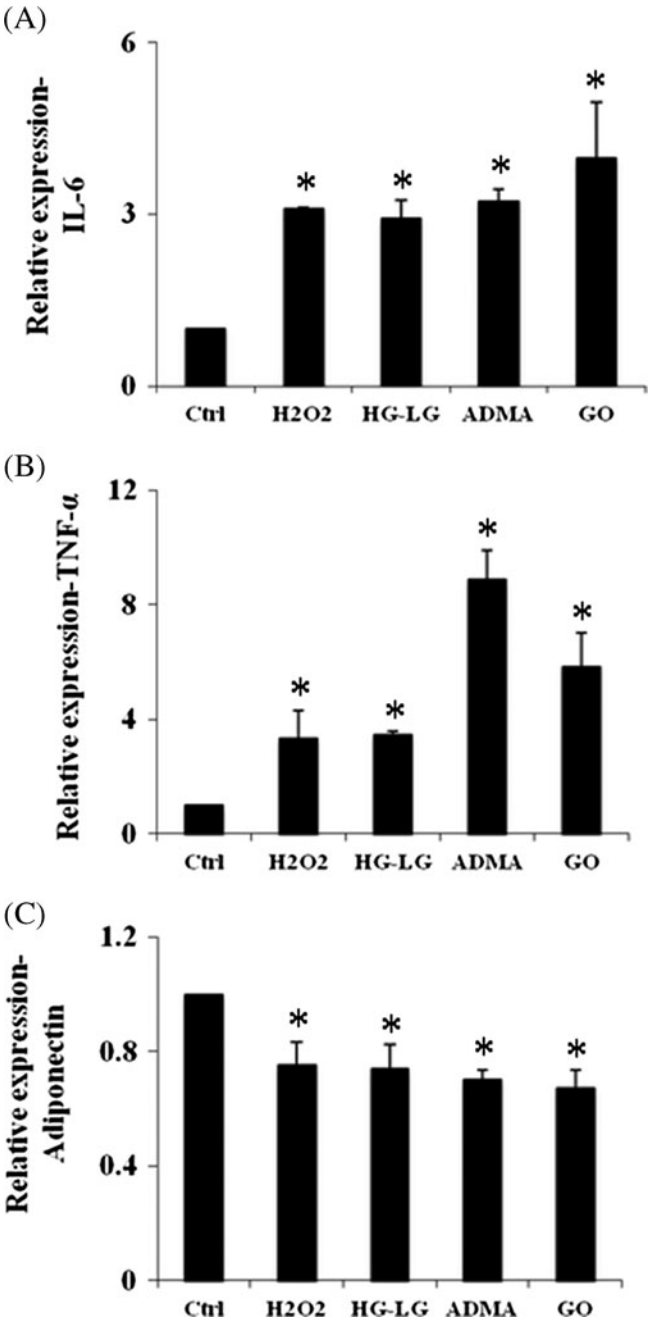


**Figure 5.** Real-time PCR gene expression patterns (mean±SE) of adipokines viz IL-6 (**A**), TNFα (**B**), and adiponectin (**C**), from 3T3-L1 adipocytes under different experimental conditions. *$p<0.01$ compared to control.

blots of senescent markers are presented in figure 4A. Compared to control cells, cells imposed for oxidative stress also exhibited increased protein expression of p53 (figure 4B) and p21 (figure 4C). Since senescence-like changes might be associated with increased expression of pro-inflammatory cytokines, we next examined the mRNA and protein expression of adipokines in the adipocytes subjected to various treatments. Cells treated for oxidative stress conditions exhibited significantly increased mRNA expression of pro-inflammatory signals, viz IL-6 (figure 5A) and

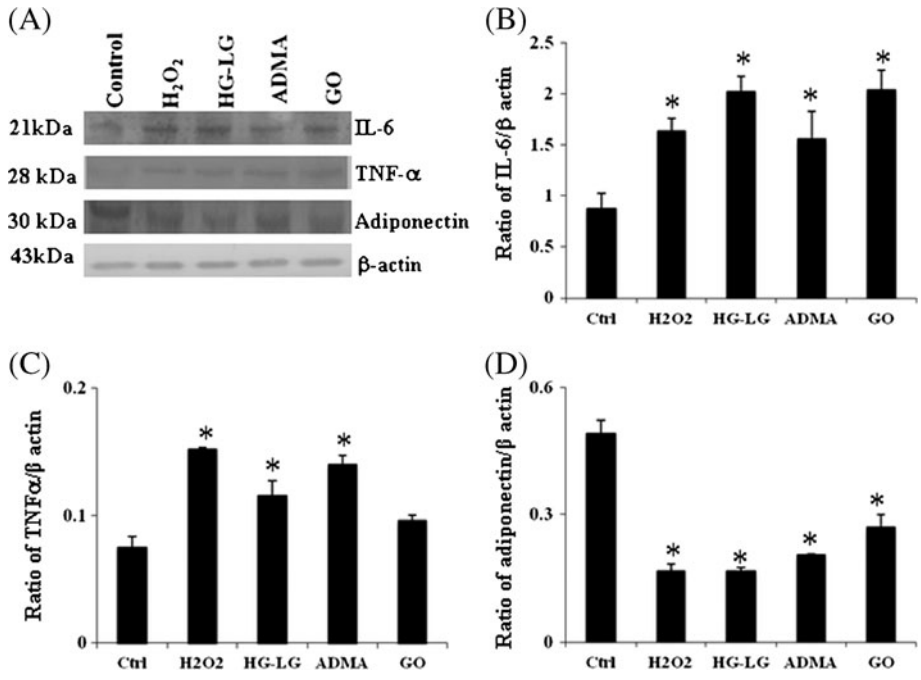


**Figure 6.** Protein expression patterns of adipokines. (**A**) Representative protein expression blots of adipokines along with β-actin. Cumulative protein expression data (mean±SE) of IL-6 (**B**), TNFα (**C**) and adiponectin (**D**) from 3T3-L1 adipocytes under different experimental conditions. *$p<0.05$ compared to control.

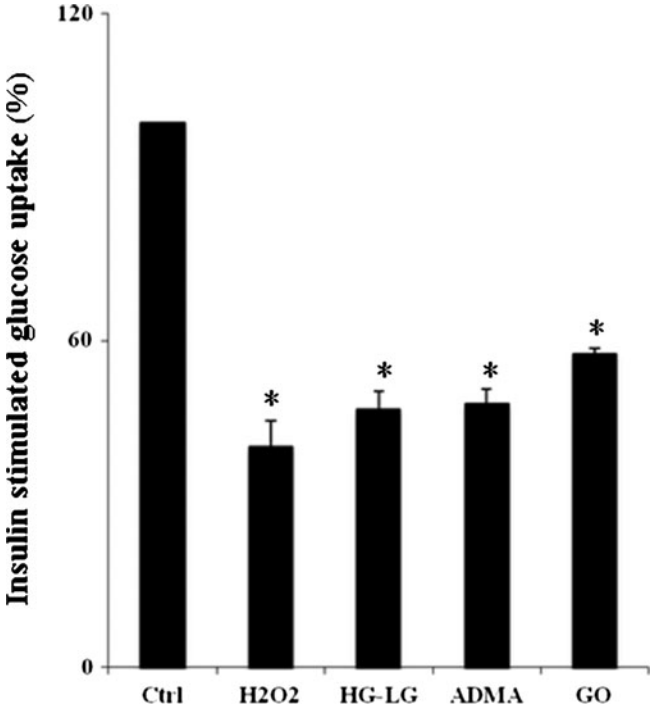


**Figure 7.** Insulin-stimulated glucose uptake (mean±SE) from 3T3-L1 adipocytes under different experimental conditions. *$p<0.001$ compared to control.

TNFα (figure 5B) and decreased mRNA expression of adiponectin (figure 5C). Representative protein blots of adipokine markers were presented in figure 6A. Consistent with the mRNA profiles, cells under stress conditions also exhibited increased protein expression of IL-6 (figure 6B), TNFα (figure 6C) and decreased adiponectin protein (figure 6D). Since increased secretion of pro-inflammatory cytokines and decreased secretion of adiponectin by adipose tissue exacerbates insulin resistance, we probed the status of insulin-stimulated glucose uptake in adipocytes treated under various test conditions. Compared to control cells, adipocytes subjected to oxidative stress not only switched to proinflammatory/senescent phenotypes but also exhibited decreased levels of insulin-stimulated glucose uptake (figure 7), implying their insulin-resistant state.

## 4. Discussion

There is an upsurge in the prevalence of age-related diseases such as type 2 diabetes mellitus and associated metabolic diseases. In fact, diabetes mellitus has recently been considered as a cause of accelerated aging (Morley 2008). Despite the fact that senescence in adipocytes could have profound clinical consequences because of the large size of the fat organ and its central metabolic role, there are only very few studies that have looked at the senescence mechanisms in

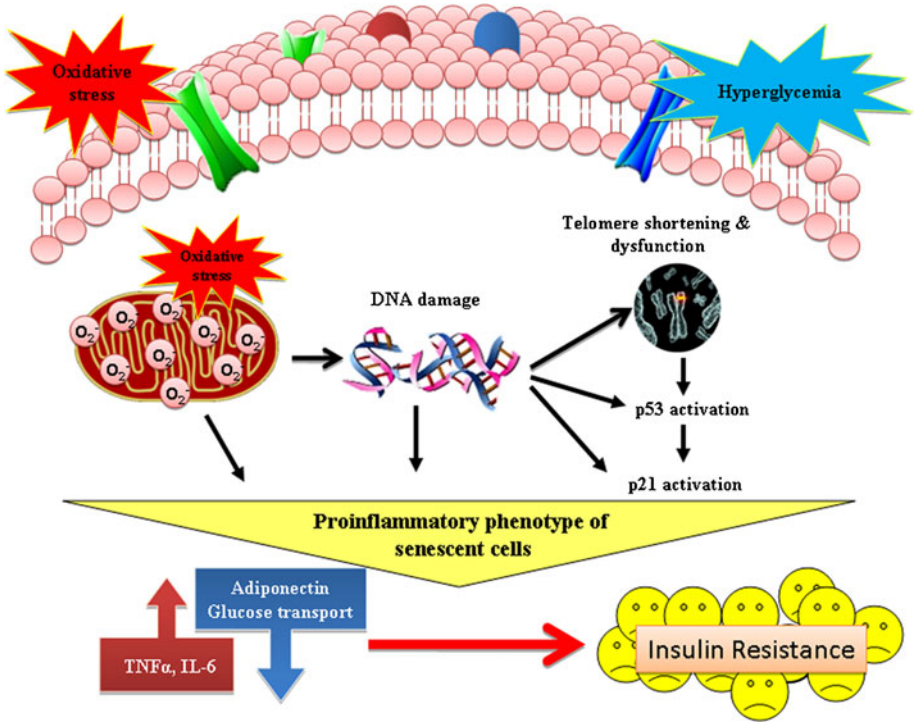


**Figure 8.** Illustration showing a tight connection among oxidative stress, shortened telomeres, augmentation of senescent signals (p53, p21), pro-inflammation and insulin resistance in adipocytes.

adipocytes (Tchkonia *et al.* 2010). In order to fulfill the research lacunae, our study in nutshell demonstrates the following: Adipocytes exposed to oxidative stress by different experimental maneuvers were characterized by shortened telomeres, senescence, pro-inflammation and functionally compromised with impairment in insulin-stimulated glucose uptake.

Cellular senescence can be triggered by telomere shortening as well as a variety of stresses and signalling imbalances (Herbig *et al.* 2004). One of our significant findings is that adipocytes exposed to oxidative stress showed shortened telomeres, augmented p53 and p21 signals, pro-inflammation and impaired insulin-stimulated glucose uptake. Indeed, p53 has been shown to play a crucial role in the regulation of insulin resistance in adipose tissue (Minamino *et al.* 2009). The adipose tissue of genetically obese mice suffering from insulin resistance exhibited features of premature aging and inflammation. These senescence-like changes were manifested by increased expression of SA-β-gal, elevated p53 levels and high expression of pro-inflammatory cytokines. Inhibition of p53 in the adipose tissue decreased the inflammation and improved insulin sensitivity (Ahima 2009; Minamino *et al.* 2009). Consistent with the animal model study, Minamino *et al.* (2009) have also demonstrated that adipose tissue from patients with diabetes showed increased SA-β-gal activity, higher levels of p53 and inflammatory markers, suggesting that aging of fat cells has a major role in human diabetes. In our study, decreased TERT mRNA expression was seen in adipocytes subjected to oxidative stress and this could be one of the causes for shortened telomeres and p53 up-regulation. In fact, ectopic expression of hTERT was shown to reduce the p53-dependent cellular stress responses (Beliveau and Yaswen 2007). Senescent and pro-inflammatory adipocytes could exert their dysregulated endocrine function by affecting various tissues. In this context, Shimizu *et al.* (2012) reported a mechanism of insulin resistance associated with heart failure that involves up-regulation of p53 in adipose tissue. These studies along with our present finding emphasize that inhibition of p53-induced adipose tissue inflammation could be an alternative therapeutic target to block the metabolic vicious cycle that occur during accelerated cellular senescence.

Senescent cells are known to secrete molecules that can alter the local microenvironment, such as pro-inflammatory cytokines (Campisi 2005; Minamino and Komuro 2007). Consistent with this we have seen up-regulation of mRNA and protein expression of pro-inflammatory cytokines such as TNFα and IL-6 along with an increase in the β-galactosidase expression in adipocytes exposed to oxidative stress. It has

been reported that increased secretion of pro-inflammatory cytokines by adipose tissue exacerbates insulin resistance in people with metabolic disorders (Hotamisligil *et al.* 1993; Kamei *et al.* 2006). In our study, adipocytes subjected to oxidative stress and senescence exhibited decreased mRNA and protein expression of adiponectin. While transgenic expression of adiponectin significantly prolonged the lifespan of normal mice (Otabe *et al.* 2007), it has been recently shown that hyperadiponectinemia protects against premature death in metabolic syndrome model mice (Otabe *et al.* 2012). Adiponectin was also shown to prevent endothelial progenitor cell senescence by inhibiting the ROS/p38 MAPK/p16 (INK4A) signaling cascade (Chang *et al.* 2010). Centenarians, a model of healthy aging and longevity, are reported to exhibit preserved insulin sensitivity as well as favourable adipokine profiles, particularly high levels of circulating adiponectin (Arai *et al.* 2011; Meazza *et al.* 2011). These studies emphasize that dysregulation of adipose-tissue-derived bioactive molecules as common ground for insulin resistance and several metabolic disorders.

It has been recently conceived that oscillations in glucose levels (glucose excursions) represent a more detrimental condition in tissue dysfunction and this has been studied well in vascular tissues. Hyperactivation of p53 was shown during glucose oscillation in HUVEC (Schisano *et al.* 2011). Our study extend these observations to adipocytes as we have seen telomere shortening, p53 activation and insulin resistance in adipocytes exposed to oscillating glucose levels. Similarly, our observation that adipocytes subjected to ADMA treatment also exhibited accelerated senescence and insulin resistance is an important finding. Increased ADMA levels were shown associated with insulin resistance (Rask-Madsen *et al.* 2010) and type 2 diabetes (Yi *et al.* 2011). Increased endothelial cell senescence was shown inducted by ADMA (Bode-Böger *et al.* 2005). ADMA reduces insulin sensitivity (Sydow *et al.* 2008) and significantly impairs both basal and insulin-stimulated glucose transport in adipocytes through activation of ROS generation (Yang *et al.* 2009). Recently, Adelibieke *et al.* (2012) have demonstrated that ADMA induces endothelial cell senescence by increasing ROS production and p53 activity. Consistent with this, our study demonstrates a role for ADMA in adipocyte cell senescence and insulin resistance.

To conclude, creating oxidative-stress-induced cellular senescence *in vitro* in an adiopocyte cell model, our study has provided evidence that there is a tight connection among shortening of telomeres, cellular senescence, augmentation of p53 and p21 signals, pro-inflammation and genesis of insulin resistance in adipocytes (figure 8). Considering the involvement of p53 polymorphism and the risk for type 2 diabetes (Burgdorf *et al.* 2011; Qu *et al.* 2011), further studies are also warranted to delineate the importance of p53 alterations and its downstream signalling in metabolic diseases. It appears that inhibition of cellular aging signals and/or rejuvenation of senescent cells in adipose tissue could be a new target for the treatment of diabetes. It is emphasized that targeting the changes in the cellular composition of adipose tissue, the underlying molecular mechanisms and the altered production of adipokines may have therapeutic potential in the management of diabetes and metabolic syndrome.

## Acknowledgements

The present work was supported by a grant from the Department of Biotechnology (DBT), India. Financial assistance through Senior Research Fellowship by the Council of Scientific and Industrial Research (CSIR), India, is also acknowledged.

## References

Adaikalakoteswari A, Balasubramanyam M and Mohan V 2005 Telomere shortening occurs in Asian Indian Type 2 diabetic patients. *Diab. Med.* **22** 1151–1156

Adaikalakoteswari A, Rema M, Mohan V and Balasubramanyam M 2007 Oxidative DNA damage and augmentation of poly (ADP-ribose) polymerase/nuclear factor-kappa B signaling in patients with type 2 diabetes and microangiopathy. *Int. J. Biochem. Cell Biol.* **39** 1673–1684

Adelibieke Y, Shimizu H, Muteliefu G, Bolati D and Niwa T 2012 Indoxyl sulfate induces endothelial cell senescence by increasing reactive oxygen species production and p53 activity. *J. Ren. Nutr.* **22** 86–89

Ahima RS 2009 Connecting obesity, aging and diabetes. *Nat. Med.* **15** 996–997

Arai Y, Takayama M, Abe Y and Hirose N 2011 Adipokines and aging. *J. Atheroscler. Thromb.* **18** 545–550

Balasubramanyam M, Adaikalakoteswari A, Monickaraj SF and Mohan V 2007 Telomere shortening & metabolic/vascular diseases. *Indian J. Med. Res.* **125** 441–450

Balasubramanyam M, Aravind S, Gokulakrishnan K, Prabu P, Sathishkumar C, Ranjani H and Mohan V 2011 Impaired miR-146a expression links subclinical inflammation and insulin resistance in Type 2 diabetes. *Mol. Cell Biochem.* **351** 197–205

Beliveau A and Yaswen P 2007 Soothing the watchman: telomerase reduces the p53-dependent cellular stress response. *Cell Cycle* **6** 1284–1287

Bode-Böger SM, Scalera F and Martens-Lobenhoffer J 2005 Asymmetric dimethylarginine (ADMA) accelerates cell senescence. *Vasc. Med.* **10 (Suppl 1)** S65–S71

Burgdorf KS, Grarup N, Justesen JM, Harder MN, Witte DR, Jørgensen T, Sandbæk A, Lauritzen T, *et al.* 2011 Studies of the association of Arg72Pro of tumor suppressor protein p53 with type 2 diabetes in a combined analysis of 55,521 Europeans. *PLoS One* **6** e15813

Campisi J 2005 Senescent cells, tumor suppression, and organismal aging: good citizens, bad neighbors. *Cell* **120** 513–522

Cawthon RM 2002 Telomere measurement by quantitative PCR. *Nucleic Acids Res.* **30** e47

Chang J, Li Y, Huang Y, Lam KS, Hoo RL, Wong WT, Cheng KK, Wang Y, *et al.* 2010 Adiponectin prevents diabetic premature senescence of endothelial progenitor cells and promotes endothelial repair by suppressing the p38 MAP kinase/p16INK4A signaling pathway. *Diabetes* **259** 2949–2959

Guarner-Lans V, Rubio-Ruiz ME, Pérez-Torres I and Baños de MacCarthy G 2011 Relation of aging and sex hormones to metabolic syndrome and cardiovascular disease. *Exp. Gerontol.* **46** 517–523

Herbig U, Jobling WA, Chen BP, Chen DJ and Sedivy JM 2004 Telomere shortening triggers senescence of human cells through a pathway involving ATM, p53, and p21(CIP1), but not p16 (INK4a). *Mol. Cell.* **14** 501–513

Hotamisligil GS, Shargill NS and Spiegelman BM 1993 Adipose expression of tumor necrosis factor-α: direct role in obesity-linked insulin resistance. *Science* **259** 87–91

Kamei N, Tobe K, Suzuki R, Ohsugi M, Watanabe T, Kubota N, Ohtsuka-Kowatari N, Kumagai K, *et al.* 2006 Overexpression of monocyte chemoattractant protein-1 in adipose tissues causes macrophage recruitment and insulin resistance. *J. Biol. Chem.* **281** 26602–26614

Lu T and Finkel T 2008 Free radicals and senescence. *Exp. Cell Res.* **314** 1918–1922

Meazza C, Vitale G, Pagani S, Castaldi D, Ogliari G, Mari D, Laarej K, Tinelli C, *et al.* 2011 Common adipokine features of neonates and centenarians. *J. Pediatr. Endocrinol. Metab.* **24** 953–957

Mehta JL, Rasouli N, Sinha AK and Molavi B 2006 Oxidative stress in diabetes: A mechanistic overview of its effects on atherogenesis and myocardial dysfunction. *Int. J. Biochem. Cell Biol.* **38** 794–803

Minamino T and Komuro I 2007 Vascular cell senescence: contribution to atherosclerosis. *Circ. Res.* **100** 15–26

Minamino T, Orimo M, Shimizu I, Kunieda T, Yokoyama M, Ito T, Nojima A, Nabetani A, *et al.* 2009 A crucial role for adipose tissue p53 in the regulation of insulin resistance. *Nat. Med.* **15** 1082–1087

Monickaraj F, Aravind S, Gokulakrishnan K, Sathishkumar C, Prabu P, Prabu D, Mohan V and Balasubramanyam M 2012 Accelerated aging as evidenced by increased telomere shortening and mitochondrial DNA depletion in patients with type 2 diabetes. *Mol. Cell Biochem.* **365** 343–350

Morley JE, 2008 Diabetes and aging: epidemiologic overview. *Clin. Geriatr. Med.* **24** 395–405

Otabe S, Wada N, Hashinaga T, Yuan X, Shimokawa I, Fukutani T, Tanaka K, Ohki T, *et al.* 2012 Hyperadiponectinemia protects against premature death in metabolic syndrome model mice by inhibiting Akt signaling and chronic inflammation. *J. Endocrinol.* **213** 67–76

Otabe S, Yuan X, Fukutani T, Wada N, Hashinaga T, Nakayama H, Hirota N, Kojima M, *et al.* 2007 Overexpression of human adiponectin in transgenic mice results in suppression of fat accumulation and prevention of premature death by high-calorie diet. *Am. J. Physiol. Endocrinol. Metab.* **293** E210–E218

Qu L, He B, Pan Y, Xu Y, Zhu C, Tang Z, Bao Q, Tian F, *et al.* 2011 Association between polymorphisms in RAPGEF1, TP53, NRF1 and type 2 diabetes in Chinese Han population. *Diabetes Res. Clin. Pract.* **91** 171–176

Rask-Madsen C, Li Q, Freund B, Feather D, Abramov R, Wu IH, Chen K, Yamamoto-Hiraoka J, *et al.* 2010 Loss of insulin signaling in vascular endothelial cells accelerates atherosclerosis in apolipoprotein E null mice. *Cell Metab.* **11** 379–389

Salpea KD, Talmud PJ, Cooper JA, Maubaret CG, Stephens JW, Abelak K and Humphries SE 2010 Association of telomere length with type 2 diabetes, oxidative stress and UCP2 gene variation. *Atherosclerosis* **209** 42–50

Sampson MJ, Winterbone MS, Hughes JC, Dozio N and Hughes DA 2006 Monocyte telomere shortening and oxidative DNA damage in type 2 diabetes. *Diab. Care.* **29** 283–289

Schisano B, Tripathi G, McGee K, McTernan PG and Ceriello A 2011 Glucose oscillations, more than constant high glucose, induce p53 activation and a metabolic memory in human endothelial cells. *Diabetologia* **54** 1219–1226

Shimizu I, Yoshida Y, Katsuno T, Tateno K, Okada S, Moriya J, Yokoyama M, Nojima A, *et al.* 2012 p53-induced adipose tissue inflammation is critically involved in the development of insulin resistance in heart failure. *Cell Metab.* **15** 51–64

Singh NP, McCoy MT, Tice RR and Schneider EL 1988 A simple technique for quantitation of low levels of DNA damage in individual cells. *Exp. Cell Res.* **175** 184–191

Sydow K, Mondon CE, Schrader J, Konishi H and Cooke JP 2008 Dimethylarginine dimethylaminohydrolase overexpression enhances insulin sensitivity. *Arterioscler. Thromb. Vasc. Biol.* **28** 692–697

Tchkonia T, Morbeck DE, Von Zglinicki T, Van Deursen J, Lustgarten J, Scrable H, Khosla S, Jensen MD, *et al.* 2010 Fat tissue, aging, and cellular senescence. *Aging Cell* **9** 667–684

Weisberg SP, McCann D, Desai M, Rosenbaum M, Leibel RL and Ferrante AW Jr 2003 Obesity is associated with macrophage accumulation in adipose tissue. *J. Clin. Invest.* **112** 1796–1808

Yang ZC, Wang KS, Wu Y, Zou XQ, Xiang YY, Chen XP and Li YJ 2009 Asymmetric dimethylarginine impairs glucose utilization via ROS/TLR4 pathway in adipocytes: an effect prevented by vitamin E. *Cell Physiol. Biochem.* **24** 115–124

Yi L, Zhang P, Ji X, Liang Y, Wang Y, Zhou Z and Chen B 2011 Quantitation of L-arginine and asymmetric dimethylarginine in human plasma by LC-selective ion mode-MS for Type 2 diabetes mellitus study. *Chem. Pharm. Bull. (Tokyo)* **59** 839–843

*MS received 11 September 2012; accepted 31 October 2012*

Corresponding editor: VEENA K PARNAIK